

# Fucosterol and Fucoxanthin Enhance Dentin Collagen Stability and Erosion Resistance Through Crosslinking and MMP Inhibition

Won Sek Lee<sup>1</sup>, Yeon Kim<sup>2</sup>, Moon-Kyoung Bae<sup>3</sup>, Kyung-Hyeon Yoo<sup>4</sup>, Hae Ryoung Park<sup>4,5,\*</sup>, Yong-Il Kim<sup>1,5,\*</sup>

<sup>1</sup>Department of Orthodontics, Dental Research Institute, Pusan National University, Yangsan, 50612, South Korea; <sup>2</sup>Department of Oral Physiology, School of Dentistry, Pusan National University, Yangsan, 50612, South Korea; <sup>3</sup>Institute of Engineering Innovation, School of Engineering, The University of Tokyo, Tokyo, 113-8656, Japan; <sup>4</sup>Department of Oral Pathology, Periodontal Disease Signaling Network Research Center (MRC), School of Dentistry, Pusan National University, Yangsan, 50612, South Korea; <sup>5</sup>Dental and Life Science Institute, Pusan National University, Yangsan, 50612, South Korea

\*These authors contributed equally to this work

Correspondence: Yong-Il Kim, Dental and Life Science Institute, Dental Research Institute, Pusan National University Dental Hospital, Yangsan, 50612, South Korea, Tel +82- 55-360-5163, Fax +82- 55-360-5154, Email kimyongil@pusan.ac.kr

**Purpose:** To evaluate the effects of fucosterol and fucoxanthin on ultimate microtensile strength ( $\mu$ UTS), dentin collagen cross-linking, erosion resistance, and matrix metalloproteinase (MMP) inhibition.

**Methods:** Dentin beams and slices were prepared from extracted human teeth and treated with concentrations of 50  $\mu$ g/mL, 100  $\mu$ g/mL, and 200  $\mu$ g/mL of fucosterol and fucoxanthin. Fourier-transform infrared spectroscopy (FTIR) was used to analyze collagen cross-linking. In situ zymography was used to quantify MMP activity inhibition. Molecular docking simulations were used to gain insights into the binding interactions between the compounds and dentin collagen/MMPs. In vitro erosion tests and 3D non-contact profilometry were used to evaluate erosion resistance.  $\mu$ UTS was measured to assess mechanical enhancement.

**Results:** FTIR analysis showed increased collagen cross-linking in fucosterol and fucoxanthin treated groups, with notable shifts in amide II bands in a concentration-dependent manner. In situ zymography revealed effective MMP inhibition in fucosterol and fucoxanthin treated samples, with inhibition increasing at higher concentrations, supporting the stabilization of the dentin matrix. Molecular docking confirmed favorable binding interactions between the compounds and both collagen and MMPs. Erosion tests demonstrated significantly reduced dentin structure loss and surface roughness in the experimental samples. Treatment with fucosterol and fucoxanthin significantly increased  $\mu$ UTS values, compared to controls, indicating enhanced dentin strength.

**Conclusion:** Fucosterol and fucoxanthin from marine algae effectively enhance dentin mechanical properties and resistance to acid-induced erosion through collagen cross-linking and MMP inhibition. These findings suggest that these compounds could serve as promising natural treatments for dentin preservation against acid attacks, potentially improving oral health outcomes.

**Keywords:** fucosterol, fucoxanthin, MMP inhibitor, collagen cross-linker, marine-derived compounds

## Introduction

Dentin is a hard dental tissue, which contributes to tooth function and health, making its preservation important to oral health outcomes. Despite its hardness, dentin is susceptible to mechanical and chemical challenges, including erosion and abrasion, which may lead to dentin exposure and hypersensitivity, and pulp degradation and abfraction.<sup>1</sup>

Dentin is structurally complex, less mineralized than enamel, and abundant in collagen. In clinical situations such as dental caries, tooth wear, or gingival recession, dentin erosion or abrasion can occur, leading to widened dentinal tubules and exposed demineralized organic matrix. Dentin organic matrix can prevent ion diffusion and minimize damage associated with acid attacks.<sup>2,3</sup> However, the exposed dentin organic matrix is susceptible to degradation by matrix metalloproteinases (MMPs), which include MMP-2, MMP-8, and MMP-9.<sup>4</sup> MMP-related degradation, which is

propagated by exposure to acidic environments that promote MMP and proteolytic activity, can be inhibited by saliva by acting as a natural buffer for pH changes.<sup>5</sup>

In addition to the inherent buffer system, various protective interventions can be used to prevent dentin erosion by promoting collagen crosslinks within the acid-etched layer of demineralized collagen matrix, which prevents collagen degradation and inhibits MMP activity. Multiple studies have shown collagen cross-linkers and MMP inhibitors such as carbodiimide, glutaraldehyde, riboflavin, epigallocatechin-3-gallate (EGCG), and proanthocyanidin improve the longevity and stability in resin-dentin bonding during dental restoration.<sup>6</sup> Additionally, some studies have shown the efficacy of natural compounds, such as flavonoids, in inhibiting MMPs.<sup>7</sup>

Zhang et al reported on the use of marine natural products as MMP inhibitors.<sup>7</sup> Among these marine-derived compounds, fucosterol (FS) and fucoxanthin (FX) have gained particular interest due to their diverse biological activities and potential applications in various fields. Both originating from marine algae, FS and FX have been shown to have antidiabetic, antibacterial, antifungal, antihyperlipidemic, and antidepressant properties, with some studies showing efficacy in dementia prevention.<sup>8–13</sup> Moreover, some studies have highlighted their inhibitory effects on osteoclast differentiation, accompanied by a satisfactory safety profile.<sup>14,15</sup> Chemically, FS is similar to sitosterol, as it possesses a tetracyclic ring structure and hydroxyl group that may react by pi-electron cloud over aromatic group and electron group of alkyl group.<sup>16–18</sup> FX, which is similar to beta-carotene, belongs to carotenoids and has isoprene units and a hydroxyl group.<sup>19</sup> Theoretically, FS and FX may inhibit MMP activity in a sitosterol- or beta-carotene-like manner. However, evidence on the effects of these compounds on MMP activity is insufficient and studies are required to understand whether these compounds can affect the mechanical properties of the demineralized collagen matrix observed during dentin erosion.

This study aimed to examine the impact of FS and FX on dentin erosion, collagen crosslinking, and MMP inhibition. Additionally, we sought to investigate the effects of these marine algae-derived compounds on the mechanical properties of demineralized dentin collagen matrix. To this end, we evaluated degree of crosslinking by FTIR and MMP inhibition by in situ zymography. Molecular docking analysis was used to evaluate the interaction between FS and FX, and MMP and collagen in silico. Finally, in vitro dentin erosion by profilometry analysis and the  $\mu$ UTS of collagen were assessed.

## Materials and Methods

### Degree of Crosslinking

The 1-mm thick dentin slices were cut perpendicular to the major axis from the mid-crown portions of 30 extracted human premolars using a low-speed diamond saw (Accutom-100, Struers, Cleveland, OH, USA) with water cooling. Four slices were obtained from each tooth. The premolars were extracted for orthodontic reasons from patients aged 18–25 years. The teeth were stored in 0.1% thymol solution at 4 °C and used within one month of extraction. Then all the slices were pulverized in liquid nitrogen into a fine powder using mortar and pestle. The dentin powder was filtered through a 25- $\mu$ m sieve and completely demineralized with 10% phosphoric acid (pH=1.0) for 5 h. The demineralized dentin powder was rinsed with deionized water by repeated centrifugation (4000 g for 10 min at 4 °C) and lyophilized using a vacuum lyophilizer. The processed powder was divided into eight groups with each group having a sample size of 4 separate powder samples (n=4 per group): (1) FS-200; (2) FS-100, (3) FS-50, (4) FX-200, (5) FX-100, (6) FX-50, (7) deionized water, and (8) ethanol. Each sample consisted of 1 mg of demineralized dentin powder. A 1-mg quantity of demineralized dentin powder was immersed in 2.5 mL of treatment solution for 10 min at room temperature and extensively washed with deionized water by centrifugation and lyophilized.<sup>20</sup>

The treated dentin powder of each sample was investigated with Fourier-transform infrared spectroscopy (ATR-FTIR, IS50; Thermo Scientific Co., Waltham, MA, USA), using a resolution of 4 cm<sup>-1</sup>, 32 scans in transmittance mode. The scan range was 4000 to 400 cm<sup>-1</sup>. The spectra range was magnified from nearly 3300 cm<sup>-1</sup> to identify the OH groups and 1800 to 900 cm<sup>-1</sup> to investigate amide I bands ( $\sim$ 1600–1700 cm<sup>-1</sup>), amide II band ( $\sim$ 1500–1600 cm<sup>-1</sup>), phosphate-related peaks ( $\sim$ 500 and  $\sim$ 1000 cm<sup>-1</sup>), and shoulder-to-dentin collagen cross-linking.

## In situ Zymography

Dentin blocks (20 mm x 15 mm x 1 mm) were cut perpendicular to the major axis from the mid-crown portions of 30 extracted human premolars with a low-speed saw (Accutom-100, Struer, Cleveland, OH, USA) under water cooling. Four slices were obtained from each tooth. The premolars were extracted for orthodontic reasons from patients aged 18–25 years. The teeth were stored in 0.1% thymol solution at 4 °C and used within one month of extraction. Then, the dentin blocks were wet-polished with 600-, 1000-, 2000-, and 4000-grit silicon carbide paper (Buehler, Lake Bluff, IL, USA). The dentin block was randomly assigned to eight groups, as previously mentioned. Each dentin block was ultrasonically cleaned, placed on glass slides, and etched with 37% phosphoric acid for 15s. After washing with air and water by a three-way syringe for 5 seconds and gently drying with air, each sample was treated with 100 µL of the respective treatment solutions for 1 min.<sup>21</sup>

Fluorogenic dye-quenched gelatine was used in situ to investigate whether FS and FX directly inhibits dentin-derived MMPs. Quenched fluorescein-conjugated gelatin (E-12055, Life Technologies Corporation, Eugene, OR) was added to the etched dentin block at 37 °C for 24 h with light protection. The amount of green fluorescence produced by the dissolved quenched fluorescein-conjugated gelatine mixture produced by MMP was observed by confocal laser microscopy (excitation/emission: 488/530 nm; CLSM) (LSM 900, Zeiss, Oberkochen, Germany). Subsequently, 85-µm thick optical sections were acquired from different focal planes, and the stacked images were analyzed, quantified, and processed with ImageJ software (NIH, Bethesda, MD, USA). 15 images per group were analyzed. The MMP inhibitory percentage was calculated using the following formula:

$$\text{Inhibitory percentage (\%)} = (1 - \text{average absorbance of treated group} / \text{average absorbance of control group}) \times 100\%.^{22,23}$$

## Molecular Docking Simulation

### Molecular Docking Between Fucosterol/Fucoxanthin and MMP

The interactions between MMP-2 (PDB IDs: 1QIB)/MMP-9 (PDB IDs: 2OW0) and FS/FX were simulated using PyRx and AutoDock Vina (<https://vina.scripps.edu/>) software.<sup>24–28</sup> The crystal structures of MMP-2 and MMP-9 were selected from the Protein Data Bank (PDB) database (<https://www.rcsb.org/>). The macromolecule was set as a rigid static entity limited in a three-dimensional mesh box to completely cover the active site of the macromolecule. The ligand in the box was treated as a flexible molecule with translational, orientational, and torsional degrees of freedom. The most probable docking location was identified by the lowest binding energy and zero RMSD with exhaustiveness of eight. The macromolecule-ligand interaction was analyzed and visualized using UCSF ChimeraX (<https://www.cgl.ucsf.edu/chimerax/>) and BIOVIA Discovery Studio (<https://www.3ds.com/products/biovia/discovery-studio>) software.<sup>29,30</sup>

### Molecular Docking Between FS/FX and Collagen

Type-I collagen (PDB IDs: 1QSU), the major organic component of dentin, was used as the receptor for molecular docking with FS/FX.<sup>31</sup> Docking simulations were performed using the PyRx and AutoDock Vina in a similar manner with the previously described method, and the most probable docking location and lowest binding energy predicted were screened.

The interactions between type-I collagen and ligand structures were analyzed using BIOVIA Discovery Studio software. Docking parameters and free binding energy values of the ligands were calculated, and macromolecule-ligand interaction analysis and visualization of collagen-ligand complex were performed; the number of docking rounds was selected as nine.

## In vitro Dentin Erosion

A total of 64 dentin slices were cut perpendicular to the major axis from the mid-crown portions of single-rooted 16 extracted human premolars using a low-speed saw (Accutom-100, Struer, Cleveland, OH, USA) with water cooling. Four slices were obtained from each tooth. The premolars were extracted for orthodontic reasons from patients aged 18–25 years. The teeth were stored in 0.1% thymol solution at 4 °C and used within one month of extraction. The dentin slices were embedded in acrylic resin (Ortho-jet, USA), using a silicon mold. All specimens were polished using 600-, 1000-, 2000-, and 4000-grit abrasive silicon carbide papers for 10s under running water (Buehler, Lake Bluff, IL, USA). Dentin

slices with 1-mm thickness were used to simulate in vitro dentin erosion. Half of the surface of each specimen was covered with two layers of anti-acid nail varnish as the reference area, and the other half was exposed as the treated area. The specimens were then randomly assigned to eight groups with each group having a sample size of 8 slices ( $n=8$  per group): FS-50, FS-100, FS-200, FX-50, FX-100, FX-200; and deionized water and ethanol, which were used as the negative controls. Then, the specimens were exposed to artificial saliva for 1 h to allow pellicle formation.<sup>5</sup>

For each cycle, the samples were treated with 5 mL of 10% phosphoric acid (pH=1.0) for 5 min. After rinsing with deionized water, the samples were immersed in artificial saliva for 1 h and thoroughly rinsed again. Subsequently, the samples were fully immersed in treatment solution for 5 min, rinsed, and stored in artificial saliva for 1 h. Three cycles were performed per day for 5 consecutive days at 37 °C (Figure 1).

### 3D Non-Contact Profilometry Analysis

After the last erosive cycle, the samples were gently pat dry and anti-acid nail varnishes were gently peeled off with acetone and water (1:1) using forceps. Dentin structure loss ( $\mu\text{m}$ ), defined as the vertical loss of dentin tissue due to erosive wear, in each specimen was measured by a 3D optical profiler (ContourX-200, Bruker, MA, USA) with 50X magnification from a reference surface to the other surface. The measurements of capture were performed with a chromatic confocal sensor with a white light axial source, a scan velocity of 2  $\mu\text{m/s}$  and a refraction index of 10,000. For each experiment, an area of 1 mm x 1 mm was obtained in the center of the sample in the same way as the baseline measurement. The average of 5 points with 0.5-mm intervals in the area was obtained.<sup>32</sup>

Roughness parameters and tooth structure loss (TSL), expressed in nanometers, were measured for the specimens. The average roughness ( $R_a$ ) is the arithmetic mean of the height of the peaks and depth of the valleys, obtained relative to the mean line value. The root-mean-square roughness ( $R_q$ ) is the height distribution relative to the mean line value. The maximum roughness depth ( $R_{\text{max}}$ ) represents the isolated profile features. The TSL is the difference in height between the unexposed (baseline) and exposed dentin surface (treated) in each group, following the removal of the anti-acid varnish. Profile measurements (1.5 mm) were taken for the unexposed and exposed areas; the depth of the height between both areas was measured in nm, with the average expressed as the TSL value for each group.

### $\mu\text{UTS}$ of Collagen

Dentin beams ( $0.8 \times 0.8 \times 10$  mm) were cut from mid-crown portions of the human third molars extracted for orthodontic reasons from patients aged 18–25 years. The teeth were stored in 0.1% thymol solution at 4 °C and used within one month of extraction. Dentin beams were cut using a low-speed saw (Accutom-100, Struer, Cleveland, OH, USA) with water cooling. A total of 30

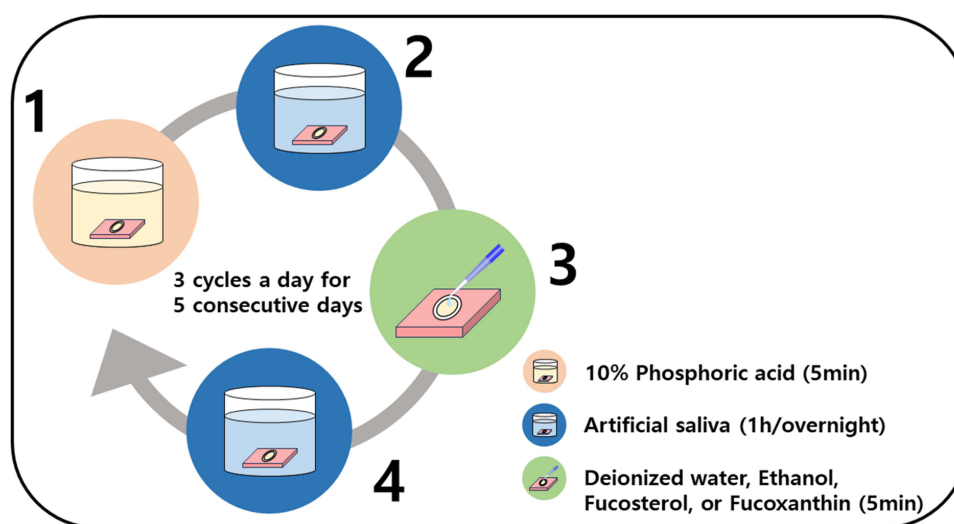


**Figure 1** Flowchart of the daily erosion cycle. (1) Sample is etched with 10% phosphoric acid for 5 min. (2) Sample is fully immersed in artificial saliva for 5 min. (3) Sample is treated with either deionized water, ethanol, fucosterol, or fucoxanthin solution for 5 min. (4) Sample is fully immersed in artificial saliva for 1 h. If it is the last step of the day, the sample is kept overnight in artificial saliva. In between steps, the sample is rinsed with deionized water, and all procedures are performed at 37 °C.

teeth were used, with 8 beams obtained from each tooth and then randomly divided into eight groups with each group having a sample size of 30 ( $n=30$ ): 50  $\mu\text{g/mL}$ , 100  $\mu\text{g/mL}$ , and 200  $\mu\text{g/mL}$  FS and FX (FS-50, FS-100, FS-200, FX-50, FX-100, and FX-200 respectively), and deionized water and ethanol as negative controls. FS and FX (Sigma-Aldrich, St. Louis, MO, USA) were dissolved in ethanol to achieve the desired concentrations. Then, the dentin beams were immersed in 10% phosphoric acid ( $\text{pH}=1.0$ ) for 5 h at room temperature. After the demineralization process, the dentin beams were rinsed with deionized water. The beams were immersed in treatment solutions for 1 h at room temperature. Subsequently, treated beams were stored in a glass petri dish to prevent sample specimen from shrinkage due to drying at room temperature in relative humidity.<sup>33</sup>

To determine the  $\mu\text{UTS}$ , each beam was adhered to the two free-sliding components of a jig mounted on a microtensile tester (T-61010K, Bisco, USA) with adhesive resin cement (U200 RX, 3M, USA). The samples were subjected to microtensile testing at a crosshead speed of 1 mm/min until rupture occurred.<sup>34</sup> The  $\mu\text{UTS}$  (MPa) was calculated according to the following formula:

$$\mu\text{UTS} = p / (b \times d),$$

where  $p$  is the maximum load (N),  $b$  is the sample width (mm), and  $d$  is the sample thickness (mm).<sup>35</sup>

## Statistical Analysis

For  $\mu\text{UTS}$ , profilometry analysis, and in situ zymography, all statistical analyses were performed using R Statistical Software (v4.3.2; R Foundation for Statistical Computing, Vienna, Austria) by using one-way analysis of variance (ANOVA) and Duncan's new multiple range test at a significance level of 0.05.

## Results

### FTIR Characterization

FTIR analysis revealed interactions between FS/FX and the collagen fibrils in the acid-treated dentin. Overall (Figure 2A), all samples showed a phosphate group related to the apatite near  $500\text{ cm}^{-1}$  and  $1000\text{ cm}^{-1}$ , as well as amide groups related to the collagen. The O-H stretching band ( $\sim 3300\text{--}3600\text{ cm}^{-1}$ ) shifted slightly to higher wave numbers for ethanol (EtOH) and FX-200 (Figure 2B). In the case of the amide groups region ( $\sim 1600\text{--}1700\text{ cm}^{-1}$ ), amide I ( $\sim 1600\text{--}1700\text{ cm}^{-1}$ ) FS/FX shifted to a lower wavenumber compared to EtOH, while amide II ( $\sim 1500\text{--}1600\text{ cm}^{-1}$ ) bands moved to higher bands with increased FS and FX concentrations (Table 1 and Figure 2C).

### In situ Zymography

Intense green fluorescence indicating gelatinolytic activity was observed in acid-etched dentin of the negative controls (deionized water and ethanol). In the treatment groups, a gradual decrease in fluorescence intensity was observed with increased treatment concentration, suggesting dentin-derived MMP activity was being inhibited (Figure 3). The inhibitory percentages by treatment groups are presented in Table 2.

### Molecular Docking Simulation

The docking simulation results for the interaction between MMP-2, MMP-9 and FS/FX are summarized in Supplementary Table 2, Supplementary Figures 1 and 2. The minimum binding energies from the nine docking results between MMP-2 and FS/FX were 8.2 and  $-8.5\text{ kcal/mol}$ , respectively. In addition, the minimum binding energies between MMP-9 and FS/FX were  $-7.1$  and  $-10.0\text{ kcal/mol}$ , respectively. The binding energies of all complexes were thermodynamically favorable, suggesting these interactions could proceed spontaneously.

The docking simulation results for the interaction between type-I collagen and FS/FX are presented in Supplementary Table 3, Supplementary Figures 3 and 4. The minimum binding energies from the nine docking results between type-I collagen and FS/FX were  $-4.4$  and  $-5.4\text{ kcal/mol}$ , respectively. Although an acceptor-acceptor interaction for type-I collagen and FX was observed, the binding energies of these complexes were thermodynamically favorable, indicating that these interactions could proceed spontaneously.



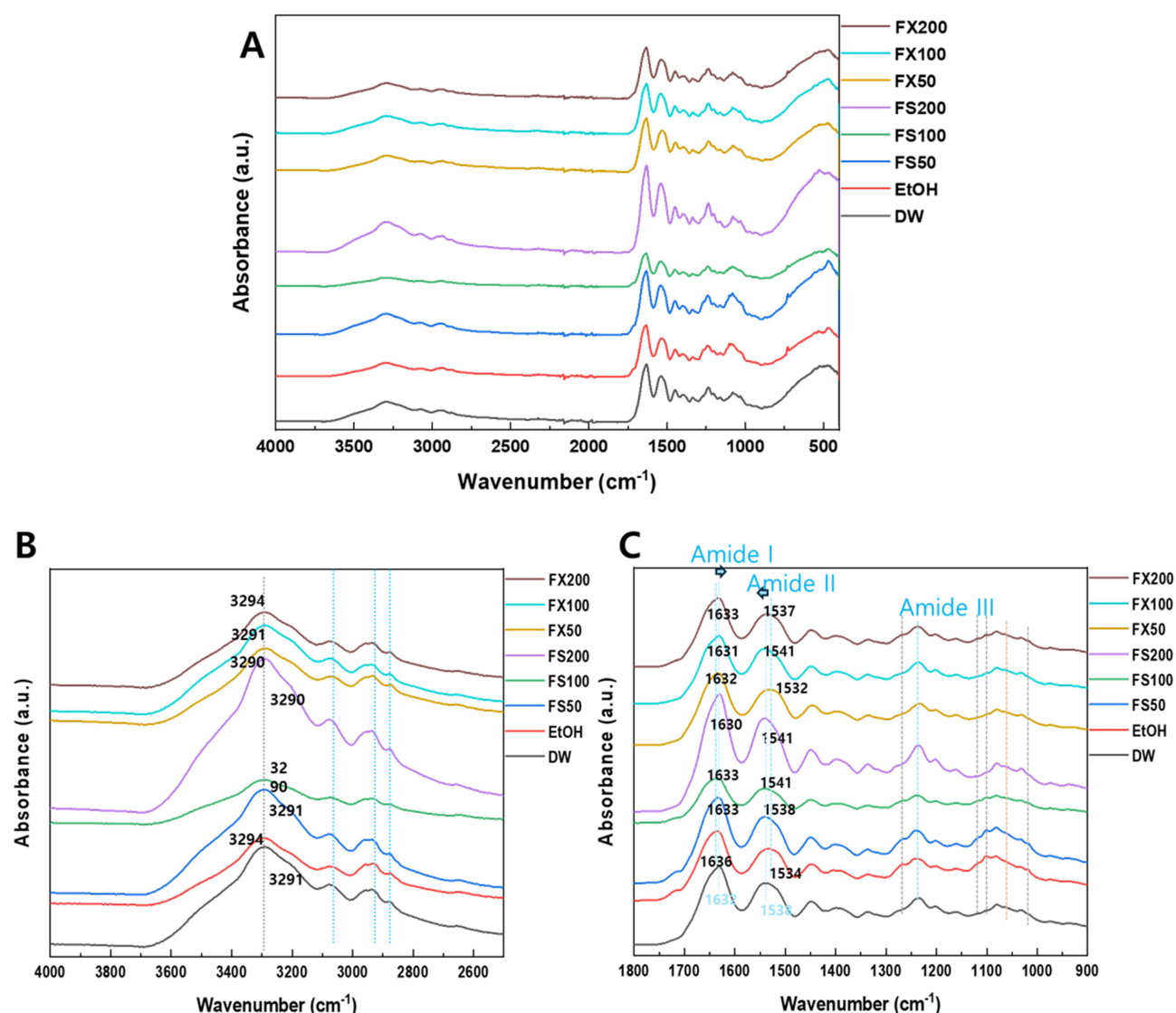


**Figure 2** FTIR spectra of demineralized dentin collagen after sample treatment with different ranges. (A) 4000–400 cm<sup>-1</sup> (B) 4000–2400 cm<sup>-1</sup> (C) 1800–900 cm<sup>-1</sup>. 50 µg/mL, 100 µg/mL, and 200 µg/mL FS and FX (FS50, FS100, FS200, FX50, FX100, and FX200 respectively).

**Abbreviations:** EtOH, Ethanol; DW, Deionized Water.

## In vitro Dentin Erosion

Figure 4 shows the erosive dentin wear of the samples treated with different solutions regarding roughness and TSL. For Ra and Rq (Supplementary Table 1), while FS-200 and FX-200 exhibited slightly higher roughness values, there were no statistically significant differences between these groups and the control. Other groups showed a decrease in these values than the control. The maximum roughness depth was comparable between the treatment and control groups. Regarding TSL, the samples treated with varying concentrations of FS and FX (FS/FX-50, 100, 200) showed less erosive dentin wear compared to the control groups, with significant differences observed for FS-200 and FX-200. The TSL values declined with increasing concentrations of FS and FX, with the least structure loss observed in the FS-200 group ( $158.68 \pm 54.79$  nm), which was significantly lower than the deionized water control ( $267.92 \pm 51.27$  nm,  $P = 0.0023$ ) and the ethanol control ( $263.38 \pm 57.92$  nm,  $P = 0.0035$ ). The FX-200 group also showed significantly lower TSL ( $196.43 \pm 60.71$  nm) compared to both controls ( $P = 0.0041$  vs deionized water,  $P = 0.0058$  vs ethanol).

**Table I** Band Shifts by Key Functional Groups

Wavenumber (cm <sup>-1</sup> )	Group	Band Shift (cm <sup>-1</sup> )
<b>O-H Stretching (~3300-3600)</b>	EtOH	3
	FS50	0
	FS100	-1
	FS200	-1
	FX50	-1
	FX100	0
	FX200	3
<b>Amide I</b>	EtOH	4
	FS50	1
	FS100	1
	FS200	-2
	FX50	0
	FX100	-1
	FX200	-2
<b>Amide II</b>	EtOH	-4
	FS50	0
	FS100	2
	FS200	2
	FX50	-6
	FX100	2
	FX200	-1

**Abbreviations:** EtOH, ethanol; FS, fucosterol; FX, fucoxanthin.

## μUTS of Collagen

The demineralized dentin beams treated with different concentrations of FS and FX exhibited significantly higher μUTS values ( $25.63 \pm 4.35$ ,  $23.94 \pm 4.17$ ,  $20.40 \pm 4.66$  MPa for FS-200, FS-100, FS-50 respectively;  $23.10 \pm 3.96$ ,  $21.41 \pm 4.87$ ,  $20.59 \pm 5.57$  MPa for FX-200, FX-100, and FX-50, respectively) than control samples ( $9.99 \pm 3.79$  MPa for deionized water and  $11.47 \pm 2.28$  MPa for ethanol) (all  $P < 0.001$  for FS-50, FS-100, and FS-200 vs deionized water and ethanol; all  $P < 0.001$  for FX-50, FX-100, and FX-200 vs deionized water and ethanol). The μUTS value of FS-200 was significantly higher than those of FS-100 and FS-50, and the μUTS value of FX-200 was significantly higher than those

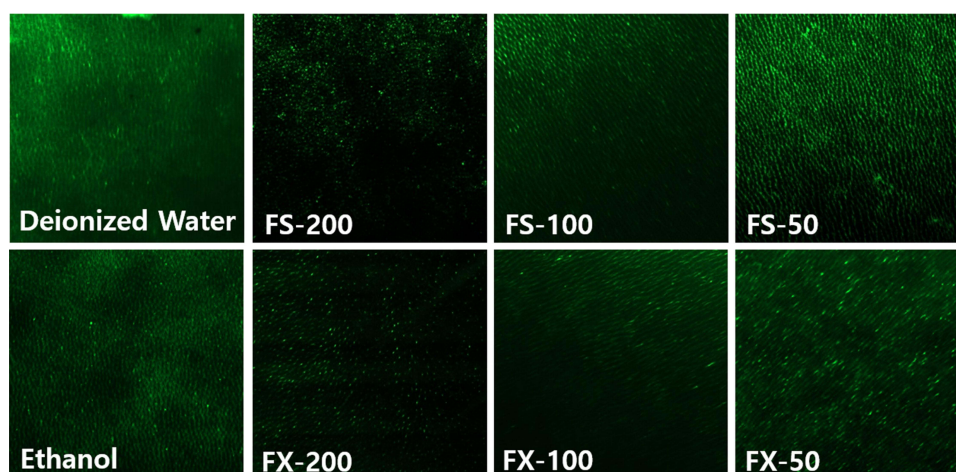


**Figure 3** Confocal Laser Microscopy (CLSM) of the in situ zymography of the group with different treatment solutions after incubation for 24 h, observed at 20X magnification. Green fluorescence represents collagenolytic activity originating from quenched FITC-conjugated collagen breakdown by MMP. Deionized water and ethanol were used as control groups. MMP fluorescent activity is shown in green. Acid-etched dentin treated with FS/FX-50, 100, and 200 resulted in weaker fluorescence, indicating reduced endogenous enzymatic activity. 50 μg/mL, 100 μg/mL, and 200 μg/mL FS and FX (FS-50, FS-100, FS-200, FX-50, FX-100, and FX-200 respectively).

**Table 2** Inhibitory Percentages by Treatment Groups

Treatment Group	Inhibitory Percentage (%)
FS-50	0.29 ± 19.94
FS-100	35.63 ± 15.31
FS-200	70.42 ± 5.72
FX-50	19.67 ± 18.25
FX-100	40.70 ± 11.94
FX-200	59.07 ± 11.73

**Abbreviations:** FS, fucosterol; FX, fucoxanthin.

of FX-100 and FX-50 (all  $P < 0.001$ , Figure 5). FS-200 and FS-100 had significantly higher values than FX at the same concentrations. There was no significant difference between FS-100 and FX-100 ( $P > 0.05$ ).

## Discussion

This study evaluated the potential of FS and FX, natural products derived from marine algae, to induce collagen crosslinking and inhibit MMP activity, thereby enhancing dentin resistance to acid challenges. Experimental results indicated that treatment with these compounds increased the  $\mu$ UTS of demineralized dentin, whose resistance to acid challenges increased in a dose-dependent manner. Molecular docking simulation provided insights into how FS and FX interact with collagen and MMPs at the molecular level.

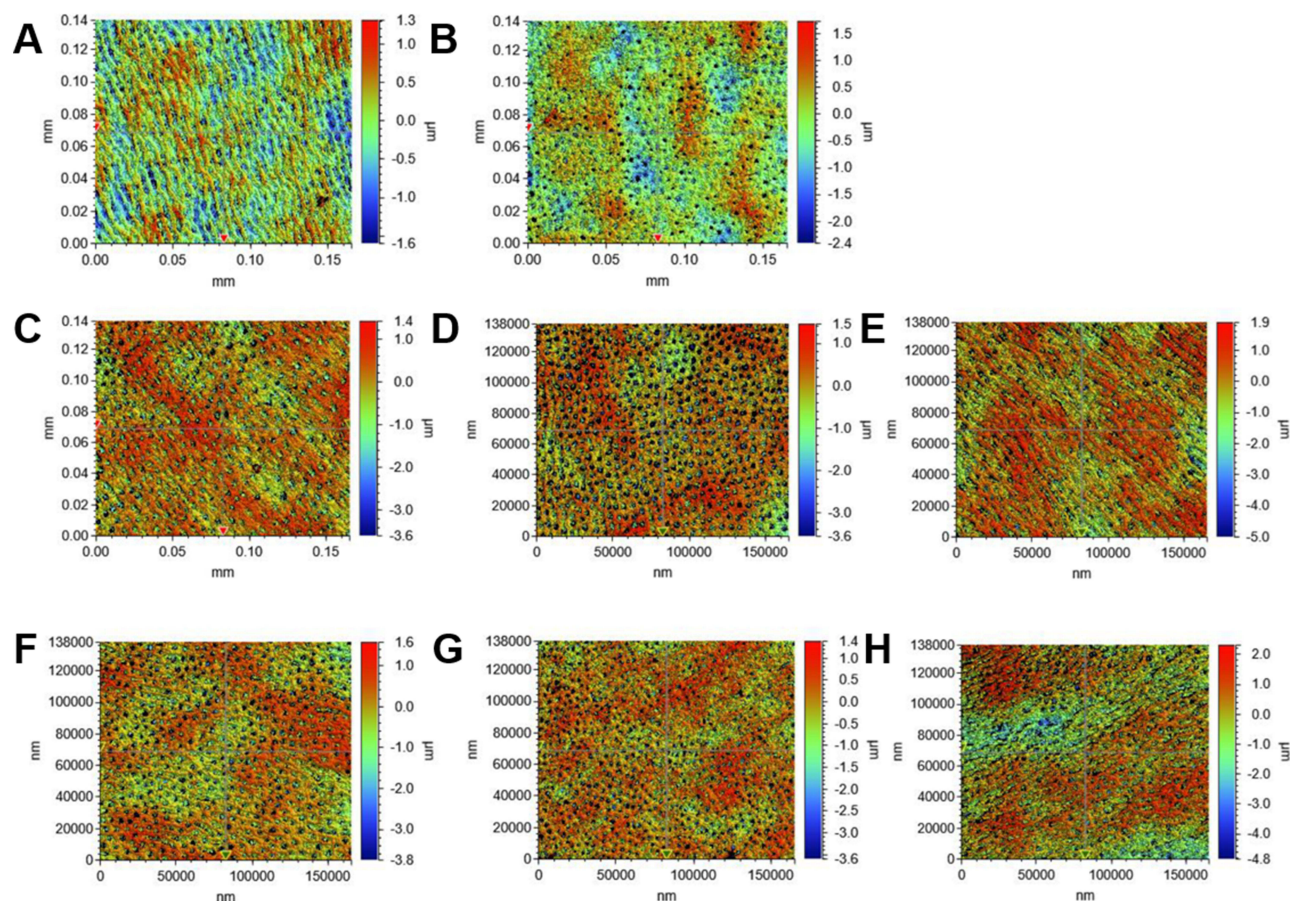


**Figure 4** 3D non-contact profilometry images showing the acid-etched dentin with different treatments. Each row represents different treatment groups: (A) deionized water, (B) ethanol, (C) FS-50, (D) FS-100, (E) FS-200, (F) FX-50, (G) FX-100, (H) FX-200. 50  $\mu$ g/mL, 100  $\mu$ g/mL, and 200  $\mu$ g/mL FS and FX (FS-50, FS-100, FS-200, FX-50, FX-100, and FX-200 respectively).



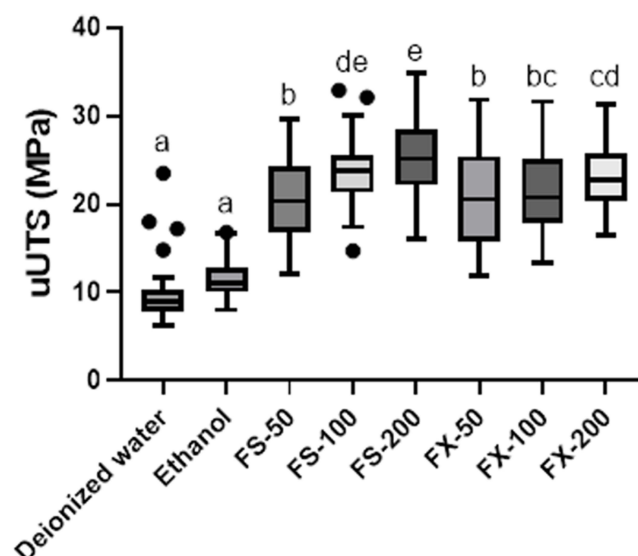


**Figure 5** Effects of fucosterol and fucoxanthin treatment on the microtensile strength of demineralized dentin beams. Same superscript letters indicate no significant difference ( $P > 0.05$ ). 50  $\mu\text{g/mL}$ , 100  $\mu\text{g/mL}$ , and 200  $\mu\text{g/mL}$  FS and FX (FS-50, FS-100, FS-200, FX-50, FX-100, and FX-200 respectively). Individual points represent outliers.

The enhancement of mechanical properties through collagen crosslinking can be attributed to several molecular-level mechanisms. Crosslinking creates additional covalent bonds between collagen molecules, restricting their relative movement and increasing the structural stability of the collagen network.<sup>36</sup> At the fibrillar level, these crosslinks help distribute mechanical loads more effectively across the collagen structure, leading to higher tensile strength.<sup>37</sup> The improved mechanical properties arise from both intrafibrillar crosslinks that strengthen individual fibrils and interfibrillar crosslinks that enhance load transfer between adjacent fibrils.<sup>36</sup> Studies have shown that increased crosslink density correlates with higher ultimate tensile strength, while also reducing the elongation at break due to molecular mobility.<sup>38</sup>

According to the FTIR results, the interaction between demineralized dentin and FS or FX may present different tendencies, helping understand the mechanisms involved in increasing dentin resistance to acid challenges. The observed spectral shifts of key functional groups suggest interactions at a molecular level and potentially indicate collagen crosslinking and stabilization. Only FX-200 showed significant differences in the O-H stretching band ( $\sim 3300\text{--}3600\text{ cm}^{-1}$ ), implying changes in hydrogen bonding interactions between the hydroxyl groups of fucoxanthin and the collagen structure. Castellan et al also indicated that such hydrogen bonding in other natural crosslinking agents, like proanthocyanidins, improve the mechanical properties of demineralized dentin.<sup>39</sup> Moreover, an increase in amide II band ( $\sim 1500\text{--}1600\text{ cm}^{-1}$ ) with increasing concentrations of FS and FX was observed. This interaction supports the mechanical and zymographic results, providing further evidence for the effectiveness of the compounds in stabilizing dentin collagen.

In this study, the C-H stretching band ( $\sim 2900\text{ cm}^{-1}$ ) and C-O stretching region ( $\sim 1050\text{--}1150\text{ cm}^{-1}$ ) showed no changes. However, the slight shift in the amide I, II, and III bands indicates that FS and FX affect collagen stability, possibly via interactions between these functional groups and collagen. These interactions can stabilize the collagen structure because the sterol of FS and the carotenoid backbone of FX may contribute to the structural stability through hydrophobic interactions with the collagen triple helix. Liu et al also reported that such hydrophobic interactions contribute to collagen stabilization in other polyphenolic compounds.<sup>40</sup> According to the simulation results and other comprehensive data, both FS and FX can react with MMP and collagen in a concentration dependent manner. Therefore, these results require further research to understand the kinetic view of interactions with collagen.

In situ zymography can help visualize the spatial distribution of enzymatic activity within tissue structures.<sup>41</sup> Herein, it revealed that after MMPs were activated in the dentin, FS and FX inhibited the degradation of FITC-labeled collagen in a concentration dependent-manner. The decrease in fluorescence indicates a reduction in gelatinolytic activity associated with MMPs in the dentin. Notably, the inhibitory percentage increased with higher concentrations of both FS and FX with higher efficacy. The observed MMP inhibition may contribute to resistance against acid-induced erosion. This inhibitory effect may

be the result of the binding of FS and FX to the catalytic domain of MMPs, as confirmed by molecular docking results. The inhibition of MMPs may increase resistance to erosion by preventing collagen degradation.

This study utilized molecular docking simulation to elucidate the molecular-level interactions between FS, FX, MMPs, and collagen, helping elucidate the mechanism of acid resistance. The *in silico* model predicted that FS and FX would spontaneously and energetically favorably bind to MMPs and type-I collagen, suggesting their potential for MMP inhibition and enhanced collagen stability. The ligand-protein complexes were stabilized through hydrogen bonding, alkyl, pi-alkyl, pi-sigma, and van der Waals interactions with specific amino acid residues. These binding patterns appear in the S1' pocket of MMPs, responsible for the degradation effect. These results are similar to the findings by Hong et al, using quercetin, which showed inhibition through hydrophobic and electrostatic interactions within the S1' pocket.<sup>42</sup> Furthermore, the FTIR results indicate the formation of cross-links between FS/FX and collagen, which is supported by the observed increase in  $\mu$ UTS values. These findings collectively demonstrate the potential of FS and FX as collagen cross-linkers. Overall, these findings suggest the potential of these compounds in interventions aimed at inhibiting MMP effects.

The profilometry results indicated that treatment with FS-200 and FX-200 on dentin slices resulted in a lower TSL, compared to that observed in the control group, after an acid challenge, suggesting a reduction in dentin mineral loss. This enhanced resistance to acid-induced erosion can be explained by the crosslinked collagen's improved structural integrity and reduced susceptibility to enzymatic degradation. The crosslinks create a more tightly packed collagen network that physically restricts access of degradative acid to vulnerable peptide bonds.<sup>37,38</sup> This resistance to acid-induced erosion appears to be due to the increased collagen cross-links and MMP inhibition properties. Previous studies have shown that MMP inhibitors, such as chlorhexidine and doxycycline, reduce dentin erosion and degradation by inhibiting the enzymatic activity that breaks down the collagen matrix.<sup>43</sup> Chlorhexidine and a gel containing EGCG act as cross-linkers of collagen, affecting both the inhibition of MMP and the resistance to erosion.<sup>36,37</sup> Thus, the increased resistance to erosion is not solely due to MMP inhibition but rather a combined effect of collagen cross-linking and MMP inhibition. These findings suggest that FS and FX have protective effects in strengthening demineralized dentin, potentially playing a valuable role in managing ongoing erosive challenges. The ability of these compounds to enhance dentin resistance to acid challenges could be particularly beneficial in cases of persistent erosive wear.

When FS and FX were applied to demineralized dentin beams, the  $\mu$ UTS significantly increased, compared to that in the control group. This increase in tensile strength suggests that the mechanical properties of dentin collagen were potentially enhanced due to additional collagen cross-link formation. This observation aligns with fundamental principles of collagen mechanics, where crosslinking density directly influences the material's ability to resist deformation under load.<sup>37</sup> Interestingly, FS-200 and FS-100 presented significantly higher  $\mu$ UTS values than FX-200 and FX-100. This difference may be attributed to the effect of alkyl group interactions, which could potentially enhance cross-linking efficiency or stability. Similar improvements in mechanical properties have been observed with other collagen cross-linkers. Liu et al reported that proanthocyanidins increased the mechanical properties of demineralized dentin through collagen cross-link formation.<sup>20</sup> Additionally, Fawzy et al demonstrated that riboflavin, when used as a cross-linker, enhanced the mechanical properties of dentin, supporting the findings of this experiment.<sup>44</sup> Our findings with FS and FX align with these previous studies, suggesting that these marine-derived compounds may act through similar cross-linking mechanisms to improve dentin's mechanical properties.

However, it is important to note that the effects of collagen stability can vary depending on the source of cross-linking agent and pH of the solution used. For example, Aydin et al found that the mechanical properties and collagen stability of dentin treated with cross-linkers depend on the source of the cross-linking agents, specifically the proanthocyanidins.<sup>45</sup> Enrich-Essvein et al reported that proanthocyanidin-functionalized hydroxyapatite nanoparticles showed similar behavior as different cross-linking agents and pH differences between treatments resulted in varying effects.<sup>46</sup> Tang et al demonstrated the effectiveness of grape seed extract as a cross-linking agent varied with concentration and pH, which affected the stability of polyphenols important for cross-linking and remineralization-promoting effects.<sup>47</sup>

Due to the *in vitro* nature of the study, this may not fully represent the complex oral environment and interactions that occur *in vivo*. Furthermore, while the study showed dose-dependent effects, optimal concentrations for clinical use were not determined. Although the *in silico* method provided insights, it is a computational method and may not perfectly reflect real-world interactions. Some insights into the mechanisms of action do not fully represent a complete interaction of how FS and FX interact with dentin and MMPs.

The results of this study provide a foundation for clinical applications, particularly in preventive dentistry. The demonstrated ability of FS and FX to enhance dentin's resistance to acid degradation suggests potential effectiveness in clinical scenarios where dentin is exposed to acidic challenges. For instance, the significant reduction in collagen degradation observed in our study could translate to improved dentin preservation in patients with exposed root surfaces or those undergoing adhesive dental procedures. In addition to the values of FS and FX as collagen cross-linkers, future research should involve studies aimed at elucidating the molecular interactions of these substances with collagen and evaluating their stability and clinical performance in human models, helping establish their potential as clinical agents. Potential applications could include FS and FX's incorporation into dental materials or topical treatments to enhance dentin resistance against acid attacks in patients with high caries risk or dentin hypersensitivity. Moreover, the effects of FS and FX on the mineral content of dentin, particularly hydroxyapatite, should be investigated to provide a more comprehensive understanding of their potential benefits.

## Conclusion

This study demonstrated that FS and FX, extracted from marine algae, may effectively inhibit MMP activity and promote collagen cross-linking, exhibiting significant acid-resistance properties in a concentration dependent manner. These findings suggest that these natural compounds could potentially contribute to the development of interventions for dentin-related issues, although further research is needed to establish their efficacy in addressing dentin hypersensitivity specifically.

## Abbreviations

μUTS, ultimate microtensile strength; EGCG, epigallocatechin-3-gallate; FS, fucosterol; FTIR, Fourier-transform infrared spectroscopy; FX, fucoxanthin; MMP, matrix metalloproteinase; TSL, tooth structure loss.

## Ethics Approval and Informed Consent

The study was reviewed and approved by the Ethics Committee of Pusan National University Dental Hospital (IRB No: 2022-02-007-002), and all methods were performed by the Declaration of Helsinki guidelines and regulations. Informed consent was obtained from all the participants.

## Acknowledgments

This work was supported by the Medical Research Center Program (RS-2018-NR031027) through the National Research Foundation of Korea.

## Disclosure

The authors report no conflicts of interest in this work.

## References

1. Heft MW, Litaker MS, Kopycka-Kedzierawski DT, et al. Patient-centered dentinal hypersensitivity treatment outcomes: results from the national dental PBRN. *JDR Clin Trans Res*. 2018;3(1):76–82. doi:10.1177/2380084417742099
2. Meurman JH, Drysdale T, Frank RM. Experimental erosion of dentin. *Scand J Dent Res*. 1991;99(6):457–462. doi:10.1111/j.1600-0722.1991.tb01054.x
3. Kleter GA, Damen JJ, Everts V, Niehof J, Ten Cate JM. The influence of the organic matrix on demineralization of bovine root dentin in vitro. *J Dent Res*. 1994;73(9):1523–1529. doi:10.1177/00220345940730090701
4. Epasinghe DJ, Yiu C, Burrow MF. Effect of flavonoids on remineralization of artificial root caries. *Aust Dent J*. 2016;61(2):196–202. doi:10.1111/adj.12367
5. Leal IC, Rabelo CS, Viana ÍEL, Scaramucci T, Santiago SL, Passos VF. Hesperidin reduces dentin wear after erosion and erosion/abrasion cycling in vitro. *Arch Oral Biol*. 2021;129:105208. doi:10.1016/j.archoralbio.2021.105208
6. Hardan L, Daoud U, Bourgi R, et al. Effect of collagen crosslinkers on dentin bond strength of adhesive systems: a systematic review and meta-analysis. *Cells*. 2022;11(15):2417. doi:10.3390/cells11152417
7. Zhang C, Kim SK. Matrix metalloproteinase inhibitors (MMPis) from marine natural products: the current situation and future prospects. *Mar Drugs*. 2009;7(2):71–84. doi:10.3390/md7020071
8. Jung HA, Bhakta HK, Min BS, Choi JS. Fucosterol activates the insulin signaling pathway in insulin resistant HepG2 cells via inhibiting PTP1B. *Arch Pharm Res*. 2016;39(10):1454–1464. doi:10.1007/s12272-016-0819-4

9. da Silva FEF, Ávila FN, Pereira NMO, et al. Semisynthesis, in silico study and in vitro antibacterial evaluation of fucosterol derivatives. *Steroids*. 2023;189:109137. doi:10.1016/j.steroids.2022.109137
10. Tyśkiewicz K, Tyśkiewicz R, Konkol M, Rój E, Jaroszuk-ściśel J, Skaliczka-Woźniak K. antifungal properties of fucus vesiculosus l. supercritical fluid extract against fusarium culmorum and fusarium oxysporum. *Molecules*. 2019;24(19):3518. doi:10.3390/molecules24193518
11. Song Y, Oh GH, Kim MB, Hwang JK. Fucosterol inhibits adipogenesis through the activation of AMPK and Wnt/ $\beta$ -catenin signaling pathways. *Food Sci Biotechnol*. 2017;26(2):489–494. doi:10.1007/s10068-017-0067-5
12. Zhen XH, Quan YC, Jiang HY, Wen ZS, Qu YL, Guan LP. Fucosterol, a sterol extracted from Sargassum fusiforme, shows antidepressant and anticonvulsant effects. *Eur J Pharmacol*. 2015;768:131–138. doi:10.1016/j.ejphar.2015.10.041
13. Gan SY, Wong LZ, Wong JW, Tan EL. Fucosterol exerts protection against amyloid  $\beta$ -induced neurotoxicity, reduces intracellular levels of amyloid  $\beta$  and enhances the mRNA expression of neuroglobin in amyloid  $\beta$ -induced SH-SY5Y cells. *Int J Biol Macromol*. 2019;121:207–213. doi:10.1016/j.ijbiomac.2018.10.021
14. Ha YJ, Choi YS, Oh YR, et al. Fucoxanthin suppresses osteoclastogenesis via modulation of MAP kinase and Nrf2 signaling. *Mar Drugs*. 2021;19(3):132. doi:10.3390/md19030132
15. Miyashita K, Hosokawa M. Fucoxanthin in the management of obesity and its related disorders. *J Funct Foods*. 2017;36:195–202. doi:10.1016/j.jff.2017.07.009
16. Zahid S, Malik A, Waqar S, et al. Countenance and implication of B-sitosterol, B-amyrin and epiafzelechin in nickel exposed Rat: in-silico and in-vivo approach. *Sci Rep*. 2023;13(1):21351. doi:10.1038/s41598-023-48772-4
17. Govindarasu M, Ganeshan S, Ansari MA, et al. In silico modeling and molecular docking insights of kaempferitrin for colon cancer-related molecular targets. *J Saudi Chem Soc*. 2021;25(9):101319. doi:10.1016/j.jscs.2021.101319
18. Narayanaswamy R, Isha A, Wai LK, Ismail IS. Molecular docking analysis of selected clinacanthus nutans constituents as xanthine oxidase, nitric oxide synthase, human neutrophil elastase, matrix metalloproteinase 2, matrix metalloproteinase 9 and squalene synthase inhibitors. *Pharmacogn Mag*. 2016;12. doi:10.4103/0973-1296.176111
19. Patil Kose AH, Potdar SN, Mishra RA, Sharma PD. In-silico investigation of phytochemicals as antiageing agents against matrix metalloproteinases using molecular docking approach. *J Plant Sci Res*. 2022;38(1):421–428. doi:10.32381/JPSR.2022.38.01.45
20. Liu R, Fang M, Xiao Y, et al. The effect of transient proanthocyanidins preconditioning on the cross-linking and mechanical properties of demineralized dentin. *J Mater Sci Mater Med*. 2011;22(11):2403–2411. doi:10.1007/s10856-011-4430-4434
21. Mazzoni A, Nascimento FD, Carrilho M, et al. MMP activity in the hybrid layer detected with in situ zymography. *J Dent Res*. 2012;91(5):467–472. doi:10.1177/0022034512439210
22. Ozcan S, Seseogullari-Dirihan R, Uctasli M, Tay FR, Pashley DH, Tezvergil-Mutluay A. Effect of polyacrylic acid on dentin protease activities. *Dent Mater*. 2015;31(8):901–906. doi:10.1016/j.dental.2015.04.018
23. Liu Z, Li F, Zhang L, Yu H, Yu F, Chen J. The effect of active components from citrus fruits on dentin MMPs. *Arch Oral Biol*. 2017;83:111–117. doi:10.1016/j.archoralbio.2017.07.006
24. Li K, Ngo FM, Yau AYL, et al. Mussel-inspired monomer - A new selective protease inhibitor against dentine collagen degradation. *Dent Mater*. 2022;38(7):1149–1161. doi:10.1016/j.dental.2022.05.002
25. Jin X, Han F, Wang Q, et al. The roles of 10-methacryloyloxydecyl dihydrogen phosphate and its calcium salt in preserving the adhesive-dentin hybrid layer. *Dent Mater*. 2022;38(7):1194–1205. doi:10.1016/j.dental.2022.06.007
26. Eberhardt J, Santos-Martins D, Tillack AF, Forli S. AutoDock Vina 1.2.0: new docking methods, expanded force field, and python bindings. *J Chem Inf Model*. 2021;61(8):3891–3898. doi:10.1021/acs.jcim.1c00203
27. Trott O, Olson AJ. AutoDock Vina: improving the speed and accuracy of docking with a new scoring function, efficient optimization and multithreading. *J Comput Chem*. 2010;31(2):455–461. doi:10.1002/jcc.21334
28. Dallakyan S, Olson AJ. Small-molecule library screening by docking with PyRx. *Methods Mol Biol*. 2015;1263:243–250.
29. Dassault Systèmes. *Discovery Studio Visualizer*. San Diego: Dassault Systèmes; 2024.
30. Pettersen EF, Goddard TD, Huang CC, et al. UCSF ChimeraX: structure visualization for researchers, educators, and developers. *Protein Sci*. 2021;30(1):70–82. doi:10.1002/pro.3943
31. Vaidyanathan J, Ravichandran S, Vaidyanathan TK, Vaidyanathan J, Ravichandran S, Vaidyanathan T. Computational analysis of adhesion of primer ligands to dentinal collagen: effect of spacer groups in ligand and amino acid residue sequence differences in collagen. *Curr Drug Discov Technol*. 2007;4(3):150–161. doi:10.2174/157016307782109689
32. Alexandria AK, Vieira TI, Pithon MM, et al. In vitro enamel erosion and abrasion-inhibiting effect of different fluoride varnishes. *Arch Oral Biol*. 2017;77:39–43. doi:10.1016/j.archoralbio.2017.01.010
33. Bedran-Russo AKB, Pereira PNR, Duarte WR, Drummond JL, Yamauchi M. Application of crosslinkers to dentin collagen enhances the ultimate tensile strength. *J Biomed Mater Res B Appl Biomater*. 2007;80(1):268–272. doi:10.1002/jbm.b.30593
34. Phrukkanon S, Burrow MF, Tyas MJ. Effect of cross-sectional surface area on bond strengths between resin and dentin. *Dent Mater*. 1998;14(2):120–128. doi:10.1016/s0109-5641(98)00018-9
35. AbuElmagd D, ElHoshy AZ, Abouauf EA. Effect of collagen cross-linkers on micro tensile bond strength of total-etch adhesive to dentin. *Egypt Dent J*. 2018;64(3):2551–2558. doi:10.21608/edj.2018.77239
36. Bou-Akl T, Banglmaier R, Miller R, VandeVord P. Effect of crosslinking on the mechanical properties of mineralized and non-mineralized collagen fibers. *J Biomed Mater Res A*. 2013;101(9):2507–2514. doi:10.1002/jbm.a.34549
37. Depalle B, Qin Z, Shefelbine SJ, Buehler MJ. Influence of cross-link structure, density and mechanical properties in the mesoscale deformation mechanisms of collagen fibrils. *J Mech Behav Biomed Mater*. 2015;52:1–13. doi:10.1016/j.jmbbm.2014.07.008
38. Koide T, Daito M. Effects of various collagen crosslinking techniques on mechanical properties of collagen film. *Dent Mater J*. 1997;16(1):1–9. doi:10.4012/dmj.16.1
39. Castellán CS, Pereira PN, Grande RHM, Bedran-Russo AK. Mechanical characterization of proanthocyanidin-dentin matrix interaction. *Dent Mater*. 2010;26(10):968–973. doi:10.1016/j.dental.2010.06.001
40. Liu Y, Chen M, Yao X, Xu C, Zhang Y, Wang Y. Enhancement in dentin collagen's biological stability after proanthocyanidins treatment in clinically relevant time periods. *Dent Mater*. 2013;29(4):485–492. doi:10.1016/j.dental.2013.01.013



41. Maravic T, Breschi L, Paganelli F, et al. Endogenous enzymatic activity of primary and permanent dentine. *Materials*. 2021;14(14):4043. doi:10.3390/ma14144043
42. Hong DW, Chen LB, Lin XJ, Attin T, Yu H. Dual function of quercetin as an MMP inhibitor and crosslinker in preventing dentin erosion and abrasion: an in situ/in vivo study. *Dent Mater*. 2022;38. doi:10.1016/j.dental.2022.09.019
43. Silva Sousa AB, Vidal CMP, Leme-Kraus AA, Pires-de-Souza FCP, Bedran-Russo AKB. Experimental primers containing synthetic and natural compounds reduce enzymatic activity at the dentin-adhesive interface under cyclic loading. *Dent Mater*. 2016;32(10):1248–1255. doi:10.1016/j.dental.2016.07.012
44. Fawzy A, Nitisusanta L, Iqbal K, Daoood U, Beng LT, Neo J. Characterization of riboflavin-modified dentin collagen matrix. *J Dent Res*. 2012;91(11):1049–1054. doi:10.1177/0022034512459053
45. Aydin B, Leme-Kraus AA, Vidal CMP, et al. Evidence to the role of interflavan linkages and galloylation of proanthocyanidins at sustaining long-term dentin biomodification. *Dent Mater*. 2019;35(2):328–334. doi:10.1016/j.dental.2018.11.029
46. Enrich-Essvein T, Rodríguez-Navarro AB, Álvarez-Lloret P, Cifuentes-Jiménez C, Bolaños-Carmona MV, González-López S. Proanthocyanidin-functionalized hydroxyapatite nanoparticles as dentin biomodifier. *Dent Mater*. 2021;37(9):1437–1445. doi:10.1016/j.dental.2021.07.002
47. Tang C, Fang M, Liu R, et al. The role of grape seed extract in the remineralization of demineralized dentine: micromorphological and physical analyses. *Arch Oral Biol*. 2013;58(12):1769–1776. doi:10.1016/j.archoralbio.2013.09.007

## International Journal of Nanomedicine

Dovepress

### Publish your work in this journal

The International Journal of Nanomedicine is an international, peer-reviewed journal focusing on the application of nanotechnology in diagnostics, therapeutics, and drug delivery systems throughout the biomedical field. This journal is indexed on PubMed Central, MedLine, CAS, SciSearch®, Current Contents®/Clinical Medicine, Journal Citation Reports/Science Edition, EMBase, Scopus and the Elsevier Bibliographic databases. The manuscript management system is completely online and includes a very quick and fair peer-review system, which is all easy to use. Visit <http://www.dovepress.com/testimonials.php> to read real quotes from published authors.

Submit your manuscript here: <https://www.dovepress.com/international-journal-of-nanomedicine-journal>